JOURNAL OF MATERIAL SCIENCE 30 (1995) 3619–3624

Wetting and adhesion of Ni–Al alloys on α-Al_2O_3 single crystals

V. MERLIN, N. EUSTATHOPOULOS
LTPCM, INP Grenoble, BP 75, D.U., 38402 Saint Martin d'Hères Cedex, France

The effect of Al additions on the wetting and adhesion of Ni on an α-Al_2O_3 single crystal was studied. Contact angles were measured by the sessile drop technique under vacuum or in He atmosphere. The morphological and chemical features of metal–vapour and metal–oxide interfaces were determined by scanning electron microscope (SEM), microprobe analysis and profilometry. The work of adhesion of Ni–Al alloys on Al_2O_3 substrates was significantly higher than for pure Ni and Al components. This result was explained by co-operative adsorption of aluminium and oxygen atoms at the Ni–Al_2O_3 interface. The influence of oxidation of the alloy on wetting and bonding is also discussed.

1. Introduction

In metal–ceramic multimaterials sessile drop experiments have a double interest. First, values of the contact angle, θ, are needed to describe liquid-state processing, for example infiltration of ceramic fibre performs by liquid metals, and secondly, by combining values of θ and surface tension of the liquid metal, σ_{LV}, the work of adhesion, W, of the metal on the ceramic can be evaluated. W is given by the Young–Dupre equation

$$W = \sigma_{SV} + \sigma_{LV} - \sigma_{SL} = \sigma_{LV}(1 + \cos\theta) \quad (1)$$

where σ_{SV} and σ_{SL} represent the solid–vapour and the solid–liquid surface energies. W, which quantifies the strength of interactions at the metal–ceramic interface, is a component of any model of mechanical properties of metal–ceramic multimaterials.

Many studies have been devoted to wetting in the pure Ni–Al_2O_3 system, as well as the effect of different alloying elements (Cr, Ti, Sn, etc.) on this property [1–4]. However, little information is available concerning the effect of Al. At low concentrations, this element enters the composition of several Ni-based super alloys while, at high concentrations, it is a basic component of Ni–Al intermetallic compounds, such as Ni_3Al and NiAl.

For the Ni_3Al compound, a point sessile drop experiment performed by Champion *et al.* [5] on α-Al_2O_3 single crystals under vacuum at 1823 K led to marginal wetting ($\theta = 83°$). Kanetkar *et al.* [6] carried out a number of sessile drop experiments under vacuum for several Ni-based alloys on different polycrystalline oxides. They observed that additions of 1 wt % Al in NiCr alloys strongly deteriorated wetting on Al_2O_3 and Y_2O_3; while, with 4 wt % Al, the detrimental effect of Al disappeared and contact angles typical of alloys without Al were found.

In this study, sessile drop experiments were performed on an α-Al_2O_3 single crystal under vacuum or inert gas atmosphere for pure Ni, Ni_3Al intermetallic and two NiAl alloys of intermediate composition. The metallic surfaces and metal–alumina interfaces were chemically and morphologically characterized by electron microprobe, SEM and interferometric profilometry. A thermodynamic analysis of Ni–Al–oxide interactions is presented and used to explain the change in θ and W with alloy composition. The mechanical behaviour of solidified drops under the thermomechanical stress produced during cooling is also discussed and correlated with interfacial features.

2. Experimental procedure

Contact angles were measured using the sessile drop method. The experiments were performed in a metallic molybdenum resistance furnace [7] fitted with two windows, enabling illumination of the sessile drop on the substrate and projection of its image on a screen. Contact angles were measured directly from the image of the drop section, with an accuracy of $\pm 2°$.

In order to reduce metal evaporation, experiments were conducted in an He atmosphere. The He gas was purified before introduction in the furnace by passing through a Zr–Al getter. The experimental atmosphere was either a dynamic vacuum of 10^{-2} Pa caused by controlled helium microleaks or a static helium pressure of 10^5 Pa. For the first mentioned atmosphere the partial oxygen pressure, $(P_{O_2})_{furnace}$, measured by an electrochemical gauge, was found to be about 10^{-12} Pa. For the static helium atmosphere the value $(P_{O_2})_{furnace} = 10^{-7}$ Pa has been estimated [4].

The temperature of the experiments was 1755 ± 15 K for pure Ni and low aluminium concentration, and 1670 ± 15 K for Ni–0.25Al alloy ($X_{Al} = 0.25$ denotes the mole fraction of Al in Ni).

TABLE I Results of sessile drop experiments for pure Ni and Ni–Al alloys on monocrystalline α-alumina

X_{Al}	Atmosphere			T (K)	θ (deg)	Drop surface	Behaviour on cooling
	Nature	Gas	P (Pa)				
0.00	Static	He	10^5		112 ± 3	Metallic	Weak bonding
0.03	Static	He + 5%H_2	10^5	1755 ± 15	95–130	Oxide layer	Strong bonding
0.08	Dynamic	He	10^{-2}		120–148	Oxide layer	Strong bonding
0.25	Dynamic	He	10^{-2}	1670 ± 15	82–106	Metallic + oxide particles	Adhesive rupture
					83 ± 3[a]		

[a] Pre-elaborated alloy.

The substrates used were cylinder platelets of monocrystalline α-alumina (sapphire of 99.993% purity). The sapphire surface had a random crystallographic orientation. After mechanical polishing, the average roughness measured by a computer-assisted interferometer was $R_a = 2$ nm. Before the experiments, the substrates were ultrasonically cleaned in acetone and then annealed under vacuum at 1473 K for 2 h in order to eliminate any hydroxyl groups that may have adsorbed on the surface. About 150 mg drops of alloys were formed by melting *in situ* nickel and aluminium on the substrate. Metals were mechanically cleaned just before experimentation. Ni contained 20 p.p.m. metallic impurities and an equal concentration of oxygen; while Al contained 5 p.p.m. metallic impurities and less than 1 p.p.m. oxygen. An experiment was conducted with an Ni–0.25Al alloy pre-elaborated on a sapphire substrate in the same furnace under He microleaks.

The experiments consisted of monitoring the time-dependent variation in contact angle as the liquid spread out on the substrate at a constant temperature. Holding periods lasted for about 20 min, this time being sufficient to obtain steady angles in the system studied. By simultaneously measuring the contact angle, the base diameter, d, and the height, h, of the drop, it is possible to check that the angles measured are advancing angles (a true decrease in θ is observed when d increases and h decreases).

After cooling the metal–alumina interface was chemically and morphologically characterized by means of microprobe analysis and SEM, respectively. When the solidified drops did not adhere to the substrate, an interferometer was used to record the shape of the ceramic surface after metal contact.

3. Results

Results on contact angles are given in Table I. The value θ = 112 ± 3° was obtained for pure Ni under purified He. This is in good agreement with the value of 109° measured at the same temperature under high vacuum [8]. However, in the latter case, evaporation of Ni caused an apparent decrease in θ with time.

After cooling, the surface of the drop has a metallic reflection and there is no detectable oxide on SEM observation. The solidified drop adhered to the substrate. However, sometime during preparation of the samples for SEM (cutting, polishing, etc.) decohesion occurred just between the metal and the substrate,

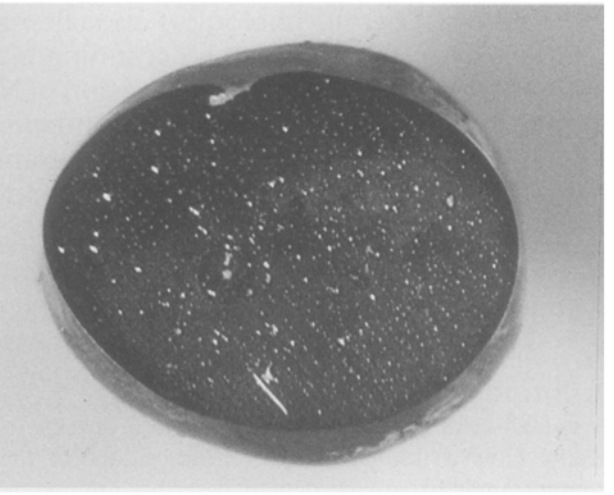

Figure 1 Base of a solidified Ni–0.03Al drop adhered to an alumina single crystal as observed through the transparent substrate (× 15). The drop base is black. Part of the surface drop is also seen in grey. The dissymmetrical wetting is due to oxidation.

i.e. by adhesive rupture. For this reason bonding of Ni on Al_2O_3 has been characterized as "weak".

Additions of Al in Ni have two opposing effects on wettability. For higher additions (mole fraction $X_{Al} = 0.25$), the wettability is improved. The contact angles obtained were in fact 30° lower than with pure Ni. For lower Al additions the wettability is worse. The drops are highly dissymmetrical as indicated by the minimum and maximum θ values observed along the solid–liquid–vapour triple line (Table I), Fig. 1.

After cooling, the surface drops of Ni–0.03Al and Ni–0.08Al alloy are covered by a matt oxide film. On the other hand, the surface of Ni–0.25Al drops has a metallic aspect. Even in this case, however, SEM characterization of the drop surface shows some oxide particles (about 0.5 μm in diameter) next to clean metallic areas (Fig. 2). When these oxide particles are situated near the triple line, they may pin it and lead locally to higher contact angles (Fig. 3).

After cooling, adhesion is strong for Ni–0.03Al and Ni–0.08Al alloys (Fig. 4), but not for Ni–0.25Al alloys for which interfacial rupture occurred. In the latter case, analysis by energy dispersion confirms that there is no trace of nickel on the substrate surface previously covered by the drop. SEM observations of the drop base showed no trace of oxide. Observation of the substrate surface shows dissolution of alumina over a depth of about 50 nm in the Ni–0.25Al alloy (Fig. 3), more pronounced near the triple line. This phenom-

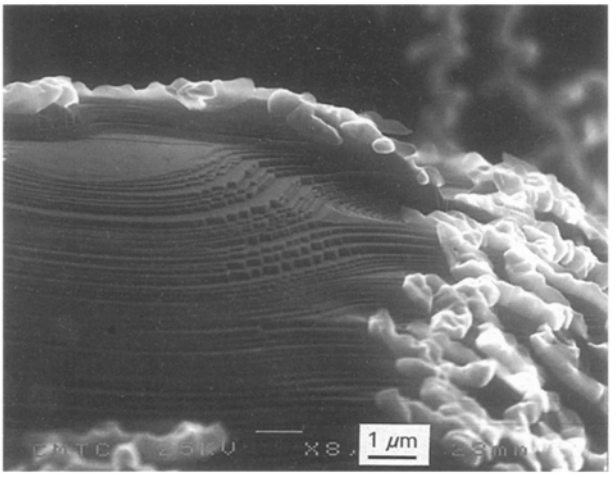

Figure 2 Surface of a solidified Ni–0.25Al drop (SEM). Oxide particles in white are clearly apparent next to metallic areas.

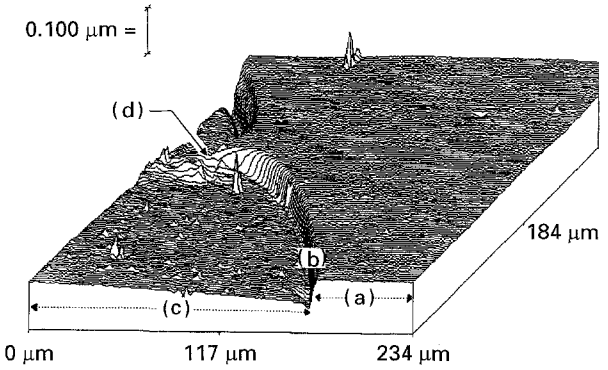

Figure 3 Topography of the α-alumina surface after interaction with Ni–0.25Al. Region (a) corresponds to the substrate surface in front of the drop, region (b) to the surface under the drop; (c) indicates the position of the triple line and (d) pinning of the triple line by oxide particles.

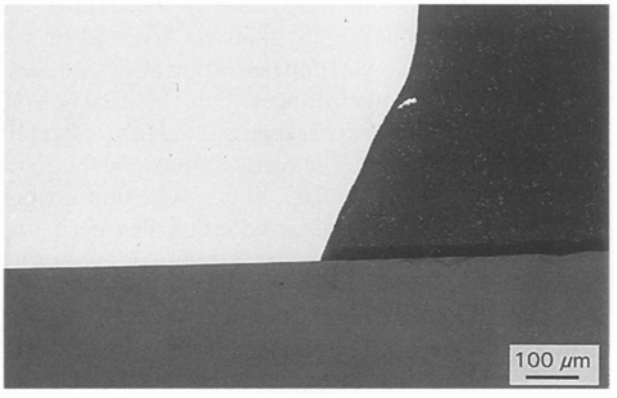

Figure 4 Cross-section of an Ni–0.03Al drop (white) on α-alumina (grey) : the interface is strong despite oxidation, indicated by non-wetting (SEM).

enon is similar to the reaction rings originally observed in the Al–Al_2O_3 system [9].

4. Discussion

4.1. Thermodynamics

The chemical interactions between an Ni–Al alloy and alumina are described by dissolution equilibrium of alumina in the alloy:

$$Al_2O_3 \rightarrow 2(Al) + 3(O) \quad (2)$$

where (Al) and (O) are dissolved aluminium and oxygen in the liquid Ni. The thermodynamic equilibrium condition for Equation 2 is written as

$$RT \ln(a_{Al}^2 \times a_O^3) = \Delta G_f^0(T) \quad (3)$$

where $\Delta G_f^0(T)$ is the standard Gibbs' energy of formation of alumina, a_{Al} is the thermodynamic activity of Al in the alloy (reference state: pure liquid Al) and a_O is that of dissolved oxygen (reference state: pure gaseous oxygen at a pressure of 0.1 MPa). For small values of mole fractions, X_{Al} (< 0.1), the activity coefficient, γ_{Al}, is approximately constant (Henry's law)

$$RT \ln\gamma_{Al} = \overline{\Delta G}_{Al(Ni)}^{E_\infty} \quad (4)$$

where $\overline{\Delta G}_{Al(Ni)}^{E_\infty}$ is the partial Gibbs energy of mixing at infinite dilution of Al in Ni.

This approximation is not true for oxygen because of strong interactions between dissolved Al and O atoms in Ni. These interactions are taken into account by the following expression

$$\ln\gamma_O = \overline{\Delta G}_{(O)Ni}^{E\infty}/RT + \varepsilon_{Al-O} \times X_{Al} + 1/2\,\rho_{Al-O} \times X_{Al}^2 + \ldots \quad (5)$$

where $\overline{\Delta G}_{(O)Ni}^{E\infty}$ is partial Gibbs' energy of mixing at infinite dilution of O in Ni. The quantities ε_{Al-O} and ρ_{Al-O} are first and second order Wagner interaction parameters between O and Al solutes in Ni. The values of $\varepsilon_{Al-O} = -210$ and $\rho_{Al-O} = 2400$ at $T = 1873$ K [10] indicate very strong interactions between Al and O atoms dissolved in the Ni matrix. Combining Equations 3, 4 and 5 and using the data in Table II and the above ε and ρ values, the variation of X_O with X_{Al} is obtained and plotted in Fig. 5. In this semi-quantitative calculation any change with temperature of ε and ρ parameters was neglected. In the Ni–Al_2O_3 system, the equilibrium values of X_O and X_{Al} are given by the point N, intersection of the curve A and the straight line B, representing the stoichiometric dissolution of alumina ($3X_{Al} = 2X_O$).

For any value of X_{Al} in the Ni–Al alloy, when X_{Al} increases, aluminium activity, a_{Al}, increases and oxygen activity, a_O, decreases in proportion to $a_{Al}^{-2/3}$ (see Equation 3). For low X_{Al} values in the Ni–Al alloy, the oxygen solubility, X_O, also decreases. But for $X_{Al} > 5 \times 10^{-3}$, X_O increases rapidly as a result of strong Al–O interactions. Thus, for alloys rich

TABLE II Values of partial Gibbs' energy of mixing of Al[a] and O_2[b] at infinite dilution in Ni and of standard Gibbs' energy of Al_2O_3 formation[c] used to calculate the curve on Fig. 5 and values of Table III

Reaction	Gibbs' energy (kJ mol^{-1})		
	$T = 1650$ K	$T = 1750$ K	Ref.
$Al = (Al)_{Ni}$[a]	− 84	− 81	[11]
$1/2\ O_2 = (O)_{Ni}$[b]	− 24	− 20	[12]
$2Al + 3/2O_2 = Al_2O_3$[c]	− 1150	− 1118	[13]

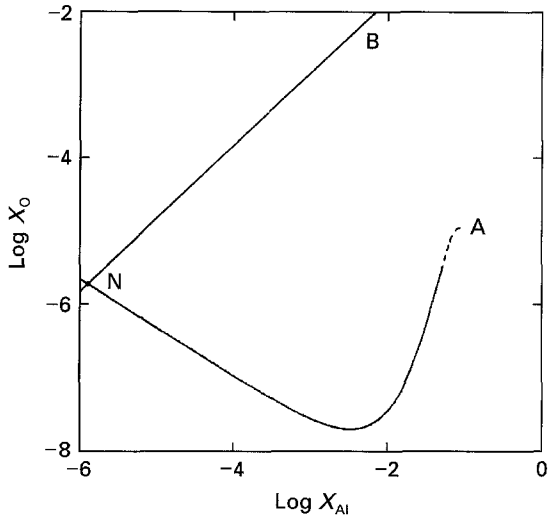

Figure 5 Calculated values of oxygen dissolved mole fraction in the Ni–Al alloy as a function of Al mole fraction, $T = 1650$ K, logarithmic scale (curve A). The straight line B represents the stoichiometric disssolution of alumina.

TABLE III Equilibrium partial pressure of O_2 and Al_2O at the liquid–solid–vapour triple line and mole fraction of oxygen dissolved in the alloy calculated for $X_{Al} = 0.01$ and 0.25

T(K)	X_{Al}	P_{Al_2O}(Pa)	P_{O_2}(Pa)	X_O
1650	0.01	10^{-4}	10^{-13}	3×10^{-8}
	0.25	10^{-1}	2×10^{-16}	$\cong 10^{-4}$
1750	0.01	5×10^{-4}	5×10^{-12}	1.6×10^{-7}
	0.25	5×10^{-1}	4×10^{-15}	$\cong 5\times10^{-4}$

in Al, the value of X_O fixed by Equilibrium 2 may be higher than in pure Ni: for such alloys, dissolution of alumina will be enhanced by aluminium additions.

At the drop surface, dissolved oxygen can combine with Al to produce volatile suboxides, mainly Al_2O, according to the reaction

$$(O) + 2(Al) \rightarrow Al_2O[G] \quad (6)$$

Thus, the overall reaction of alumina with the liquid alloy is the addition of Equation 2 and 6, i.e.

$$Al_2O_3 + 4(Al) \rightarrow 3Al_2O[G] \quad (7)$$

As the thermodynamic variance of Equation 7 is two, at fixed T and X_{Al}, the variables P_{O_2}, X_O and P_{Al_2O} are fixed too. Some calculated values of these variables are given in Table III where the X_O values have been converted into equivalent P_{O_2} values by writing $P_{O_2} = (\gamma_O \times X_O)^2$.

This Equation 7 is responsible for the corrosion of Al_2O_3 by liquid alloy. It would occur preferentially at the solid–liquid–vapour triple line where no diffusion is required to eliminate dissolved oxygen by Equation 6. This is in agreement with experimental observations, as illustrated by Fig. 3.

4.2. Contact angles and thermodynamic adhesion

The measured contact angle of pure Ni on α-alumina is in good agreement with the results given in the literature which lie in the range 107–111° at temperatures close to 1773 K (Table IV). These values do not seem to vary significantly with the furnace atmosphere (high vacuum, H_2, inert gas) or with the orientation of the alumina substrate.

TABLE IV Contact angles of pure Ni on monocrystalline α-alumina

T(K)	Atmosphere	Orientation of surface	θ(deg)	Ref.
1773	HV[a]	$10\bar{1}2$	108	[2]
1773	HV, Ar, H_2	$10\bar{1}2$	109 ± 2	[3]
1773	HV	0001	110	[14]
1853	Ar	Not specified	107	[15]
1755	HV	Random	109 ± 2	[8]
1755	He	Random	112 ± 3	This work

[a] HV, high vacuum.

Additions of aluminium in nickel have two opposing effects: at low aluminium concentrations ($X_{Al} = 0.03$ or 0.08), the aluminium leads to a higher contact angle than for pure Ni. But at high Al concentration, the contact angle is significantly lower than for pure Ni. Large non-wetting angles ($\theta \gg 90°$) obtained for low Al additions are obviously due to an oxide film on the drop surface inhibiting wetting, as also observed for pure Al [16] and aluminium alloys (for example Sn–Al–Al_2O_3 [17]). This oxide film is also responsible for the drop dissymmetry leading to significant variations of θ along the triple line. According to the work of Laurent *et al.* [16] for the pure Al–Al_2O_3 system, a fragmented thin oxide film can be eliminated under vacuum through Equation 7. The condition for such a mechanism to be effective is that the evaporation flow of oxygen, proportional to P_{Al_2O}, is higher than the impinging flow of O_2, proportional to $(P_{O_2})_{furnace}$. As shown by the values in Table III, this condition is always verified in the furnace, where $(P_{O_2})_{furnace}$ is lower than 10^{-7} Pa. Moreover, the deoxidation time varies according to $1/P_{Al_2O}$. Thus, if a time, t, equal to 10^3 s is needed to deoxidize an Ni–0.25Al alloy, then more than 10^5 s would be required for the two low Al concentration alloys studied. Obviously, this is much longer than the duration of normal sessile-drop experiments (roughly 30 min). However, the use of a reducing atmosphere, as in experiments with $X_{Al} = 0.03$, limits oxidation during temperature rises. Partial deoxidation has been obtained for this alloy leading locally to $\theta = 95°$. For this alloy, the value of 95° is therefore an upper limit of the equilibrium contact angle value. This reduction–evaporation mechanism can explain the observation that the higher the Al concentration in the alloy, the easier the deoxidation becomes. However, this observation is also compatible with a mechanism based on simple dissolution of the oxide film in liquid (Equation 2). Indeed, it can be seen from the data in Table III, that additions of Al significantly enhance oxygen solubility in the alloy.

The previous analysis helps to explain the results obtained by Kanetkar *et al.* [6] for wetting of Ni-based alloys on various oxide substrates, where the strong increase in θ observed with low Al additions (1 wt %) in Ni–Cr alloys from 85 to 135° is obviously

TABLE V W values at $T = 1750$ K calculated using the authors experimental θ values for pure Ni and Ni–Al alloys, except for pure Al [19]. σ_{LV} values are from [18]

X_{Al}	θ(deg)	σ_{LV}(mJ mol^{-1})	W(mJ mol^{-1})
0.00	112	1750	1100
0.03	95	1720	1570
0.25	83	1570	1760
1.00	65	750	1070

due to oxidation of the drops. At higher Al concentrations, dissolution of the oxide film (Equation 2) followed by evaporation of oxygen as Al_2O (Equation 6) can occur.

It may be concluded that under conditions avoiding the effect of oxide film on wettability (using high vacuum or reducing gas atmosphere or mechanical disruption of the oxide), aluminium, even at low concentration, significantly improves wetting of Ni on alumina. Moreover, using σ values from [18], θ values are converted into W values (Table V). The W values of the alloys are clearly higher than the values of both pure Ni and Al.

The intrinsic effect of Al on θ and W will be discussed using the model of Li *et al.* [20]. From this model, adsorption energies, E_{SL} and E_{LV}, of Al from the Ni bulk at the Ni–Al_2O_3 interface and at the Ni free surface, respectively, can be calculated. These quantities are given by Equations 8 and 9

$$E = \left(\sigma_{LV}^{Al} - \sigma_{LV}^{Ni}\right)\Omega - \left(W^{Al} - W^{Ni}\right)\Omega - m\lambda \quad (8)$$

$$E = \left(\sigma_{LV}^{Al} - \sigma_{LV}^{Ni}\right)\Omega - m\lambda \quad (9)$$

where σ_{LV}^{i} is the liquid–vapour surface tension of the pure metal i (Al and Ni); W^i the work of adhesion of i on alumina; Ω the molar interfacial area of the liquid [$\cong (V_M)^{2/3}$, V_M being the molar volume of the liquid]; m a structural parameter equal to 1/4; and λ the exchange energy of the Ni–Al alloy assumed to be a regular solution. Significant adsorption of aluminium at the Ni–alumina interface or at the Ni surface could be possible only if E_{SL} and E_{LV} are strongly negative (several tens of kJ mol^{-1} [20]).

Taking $\Omega = 4 \times 10^{+4}$ m^2 mol^{-1}, $\lambda = -96$ kJ mol^{-1} [21] and σ_{LV}^{i} and W^i the values given in Table V, it is found that $E_{SL} \cong E_{LV} \cong -16$ kJ mol^{-1}, respectively. These slightly negative values indicate a limited adsorption of Al at the Ni–alumina interface and at the Ni surface. For these values, Li's model predicts a slight decrease in θ and a negligible change in W between pure Ni and pure Al. Obviously, these predictions are in disagreement with experimental results, which indicate a strong decrease in θ and a net increase in the work of adhesion. This contradiction between model and experimental results can be removed if the effect of Al on W and θ is not attributed to interfacial adsorption of Al alone, but to the combined effect of Al and dissolved oxygen. It has recently been proposed that, for any metal–oxide combination, wetting and thermodynamic adhesion can be greatly enhanced by adding to a liquid matrix a metallic solute chosen so that it develops strong solute–solute interactions with oxygen [4]. Under this condition, which is well satisfied for Al and oxygen solutes in nickel matrix ($\varepsilon_{Al-O} \ll 0$), oxygen–metal clusters, such as OAl, can be formed and acquire an iono-covalent character as a result of charge transfer from metal to oxygen. This kind of cluster can develop Coulombic interactions with any iono-covalent ceramic and, as a consequence, it would adsorb strongly at metal–oxide interfaces.

From the above discussion it appears that the maximum value of the $W(X_{Al})$ curve can be explained by the combined adsorption of Al and O at the Ni–Al_2O_3 interface. Note that the maximum value of W isotherms has already been observed, but not explained, in previous work concerning wettability of alumina by Cu–Al [20] and Au–Si [22] alloys.

TABLE VI Values of linear thermal expansion coefficient, α, at room temperature [23]

Solid	Ni	Ni_3Al	Al_2O_3
$\alpha \times 10^6$ (K^{-1})	13.4	12.3	5.4

4.3. Mechanical adhesion

During cooling, thermomechanical stress is generated as a result of differences in thermal expansion coefficient between alumina and metallic phases (Table VI). This stress leads to interfacial fracture during cooling in Ni_3Al–Al_2O_3 and during SEM sample preparations for pure Ni–Al_2O_3. Conversely, bonding appears to be strong for both Ni–0.03Al and Ni–0.08Al alloys.

From Tables I and V, it can be seen that, when W increases from pure Ni to Ni–0.03Al alloy, bonding increases too. But for the intermetallic compound Ni_3Al, having the higher W value, no bonding is observed. Obviously, this is due to the brittle character of this compound which does not allow for stress relaxation by plastic deformation. Such deformation is possible for Ni and for Ni–Al solid solution (the maximum solubility of Al in Ni is about 20 at % at 1650 K and 10 at % at 900 K).

From the results of Table I the question of the effect on mechanical adhesion of an oxide film on metallic surfaces is raised. From the results obtained with Ni–0.08Al alloy, it can be seen that, although the oxide film inhibits wetting, the resulting bonding is strong. This can be explained by the fact that thin oxide layers on liquid metals at high temperature are easily deformable and can establish an intimate contact with the substrate without any porosity. In this case, the true physico-chemical discontinuity is not between the initial substrate surface and the oxide film on the drop, but between the oxide film and the metallic phase. On the other hand, thick oxide layers at low temperatures are brittle so that true interfaces cannot be established between the drop and the ceramic substrate: it is well known that no adhesion is observed after cooling in such cases (Fig. 6).

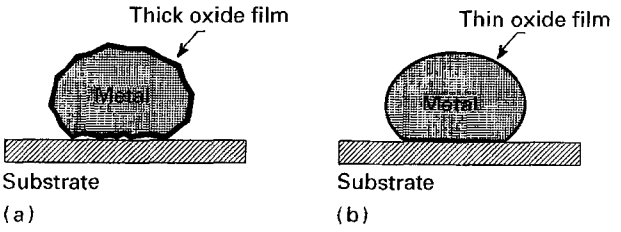

Figure 6 Schematic representation of oxidized metallic drops on a ceramic substrate in the case of thick brittle oxide film (a) and thin flexible oxide film (b). In both cases no wetting will occur, but bonding is possible only in case (b).

5. Conclusion

Al additions in Ni have two opposing effects on wettability of the Al_2O_3 substrate. At low concentrations, Al deteriorates wetting because of oxidation of the liquid alloy by this element. At high concentrations, deoxidation of the liquid alloy occurs by a dissolution–evaporation mechanism. True equilibrium contact angles of Ni–Al alloys are then measured and found to be significantly lower than the contact angle of pure Ni.

Under conditions allowing the effect of the oxide film on wetting to be avoided, Al additions to Ni lead to a rapid increase in the work of adhesion of the Ni–Al_2O_3 couple. The curve of work of adhesion versus Al mole fraction passes through a maximum which cannot be explained by simple adsorption of Al to the metal–oxide interface. Only the combined adsorption of Al and dissolved oxygen, i.e. of OAl clusters, can explain this maximum.

Despite its higher value of work of adhesion to alumina the solidified drops of intermetallic compound Ni_3Al did not adhere to the alumina during cooling, while some adhesion was observed for pure Ni. This behaviour results from the different capacity of relaxation of thermomechanical stress of ductile Ni and brittle Ni_3Al. The stronger bonding was in fact observed for Ni–Al solid solutions having high work of adhesion values (in comparison with Ni) and high ductility (in comparison with the Ni_3Al intermetallic compound).

Thin oxide films on liquid metals at high temperatures inhibit wetting, but at room temperatures do not have any detrimental effect on mechanical adhesion on oxide substrates.

References

1. C. KURKJIAN and W. KINGERY, *J. Phys. Chim.* **60** (1956) 961.
2. W. M. ARMSTRONG, A. C. D. CHAKLADER and J. F. CLARK, *J. Amer. Ceram. Soc.* **45** (1962) 115.
3. J. E. RITTER JR and M. S. BURTON, *Trans. Amer. Inst. Metal. Eng.* **239** (1967) 21.
4. P. KRITSALIS, V. MERLIN, L. COUDURIER and N. EUSTATHOPOULOS, *Acta Metall. Mater.* **40** (1992) 1167.
5. J. A. CHAMPION, B. J. KEEN and S. ALLEN, *J. Mater. Sci.* **8** (1973) 423.
6. C. S. KANETKAR, A. S. KACAR and D. M. STEPHANESCU, *Metall. Trans.* **19A** (1988) 1833.
7. I. RIVOLLET, D. CHATAIN and N. EUSTATHOPOULOS, *Acta Metall.* **35** (1987) 835.
8. V. MERLIN, Thesis, INP-Grenoble (1992).
9. J. A. CHAMPION, B. J. KEEN and J. M. SILLWOOD, *J. Mater. Sci* **4** (1969) 39.
10. Z. BUSECK, *Hulnicke Aktuality* **20** (1979) 100.
11. N. DUPIN, Phd Thesis, 1995.
12. Y. A. CHANG, K. FITZNER and M. X. ZHANG, *Progress in Mater. Sci.* **32** (1988) 97.
13. JANAF, "Thermochemical tables", Vol. 14, 3rd Edn (1985). M. W. Chase Jr., C. A. Davies, J. R. Doweny Jr., D. J. Frurip, R. A. McDonald and A. N. Syverud. National Bureau of Standards, New York, p. 161.
14. Y. V. NAÏDICH, V. S. ZHURAVLEV and V. G. CHUPRINA, *Soviet Powder Metal.* **13** (1974) 236.
15. V. A. KALMIKOV, JU. V. SVECHKOV and S. A. ELESOV, *Fizika Chimija Obrabotki Materailov* **6** (1976) 64.
16. V. LAURENT, D. CHATAIN, C. CHATILLON, N. EUSTATHOPOULOS, *Acta Metall.* **36** (1988) 1797.
17. J. G. LI, D. CHATAIN, L. COUDURIER and N. EUSTATHOPOULOS, *J. Mater. Sci. Lett.* **7** (1988) 961.
18. G. D. AYUSHIMA, E. S. LEVIN and P. V. GEL'D, *Russian J. Phys. Chem.* **43** (1969) 1548.
19. P. OWNBY, K. LI and D. WEIRAUGH Jr., *J. Amer. Ceram. Soc.* **74** (1991) 1275.
20. J. G. LI, L. COUDURIER and N. EUSTATHOPOULOS, *J. Mater. Sci.* **24** (1989) 1109.
21. A. R. MIEDEMA, F. R. DE BOER, R. ROOM and J. W. F. DORJLEIJN, *Calphad* **1** (1977) 353.
22. B. DREVET, D. CHATAIN and N. EUSTATHOPOULOS, *J. Chim. Phys.* **87** (1990) 117.
23. Y. S. TOULOUKIAN, "Thermophysical properties of matter", Vol. 12 (1975) (IFI/Plenum NW, Washington, DC, 1975) 225.

Received 10 May 1994
and accepted 3 February 1995